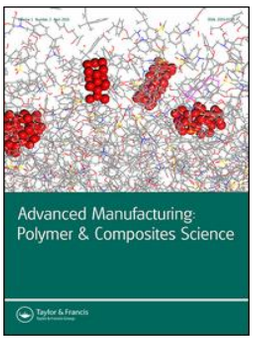

Taylor & Francis
Taylor & Francis Group

Advanced Manufacturing: Polymer & Composites Science

ISSN: 2055-0340 (Print) 2055-0359 (Online) Journal homepage: http://www.tandfonline.com/loi/yadm20

The manufacture of honeycomb cores using Fused Deposition Modeling

David Pollard, C. Ward, G. Herrmann & J. Etches

To cite this article: David Pollard, C. Ward, G. Herrmann & J. Etches (2017) The manufacture of honeycomb cores using Fused Deposition Modeling, Advanced Manufacturing: Polymer & Composites Science, 3:1, 21-31, DOI: 10.1080/20550340.2017.1306337

To link to this article: http://dx.doi.org/10.1080/20550340.2017.1306337

Published online: 26 Apr 2017.

AMPCS Advanced Manufacturing: Polymer & Composites Science

Original Research Paper

The manufacture of honeycomb cores using Fused Deposition Modeling

David Pollard*, C. Ward, G. Herrmann and J. Etches

Department of Aerospace Engineering, University of Bristol, Queens Building, University Walk, Bristol BS8 1TR, UK

Abstract Sandwich panels are used in many industries for the advantageous properties of high stiffness, good strength to weight ratio, and impact resistance. This paper investigates properties of thin-walled cores manufactured through Fused Deposition Modeling (FDM); a process which, through a wider design space, could improve the functionality of sandwich panels. The bond strength between the layers of thin walls manufactured through FDM was evaluated through tensile testing. To measure the effect of modified manufacturing speeds, wall thicknesses were varied through the flow rate and nozzle speed. Honeycomb cores using FDM were produced with different toolpaths, and compared with an example of an industry standard Nomex honeycomb core. During tensile testing, thick-walled FDM components exhibited a more ductile failure with a lower yield point when compared to thinner specimens. The ultimate tensile stress remained constant across samples within each of the tested ABS and PLA polymers used. Honeycomb cores produced using FDM were found to have a higher compressive failure force than Nomex honeycomb, and a lower specific strength. The force–displacement curves of compressive failure show a ductile response for thick specimens, consistent with the previous result. These results, combined with the increased flexibility of additive manufacture technologies, could provide a method of manufacturing high strength cores with complex geometry.

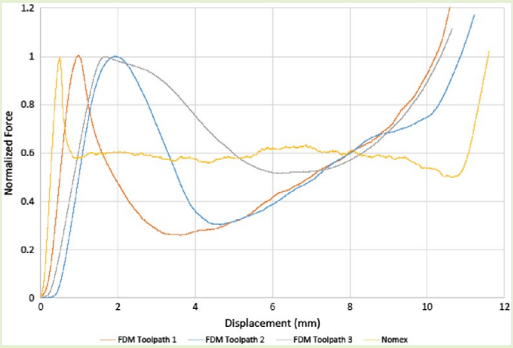

Keywords Additive manufacture, Bond strength, FDM, FFF, Thermoplastic, Honeycomb

Cite this article David Pollard, C. Ward, G. Herrmann and J. Etches: *Adv. Manuf.: Polym. Compos. Sci.*, doi:10.1080/20550340.2017.1306337

Introduction

In many industries, sandwich structures are commonly used to achieve a stiff and lightweight product within geometric constraints. In applications of these advanced composite components, core materials are placed between two face sheets of high-strength material, such as cured carbon fiber laminates. Core material choice is governed by parameters including high stiffness, good strength to weight ratio, and impact resistance.[1] Core types are divided into four categories; corrugated, cellular foams, honeycomb, and balsa wood. Within the aerospace industry, honeycomb core is a dominant choice in secondary structure applications because of the excellent mechanical properties and light weight. For panels with complex geometry, manual layup is the primary manufacturing method.[2,3]

The manufacture of sandwich panels for the aerospace industry utilizes pre-impregnated fibers (prepreg) as the face materials.[1] Complex geometries require the top face prepreg to be draped to conform to the surface; with constraints on the maximum deformation placed by the forces transferred to the core.[2] As the lateral stiffness of traditional Nomex honeycomb is a small proportion of the vertical stiffness, damage and loss of geometric accuracy may occur during this process.[3,4] In addition to this, cores are machined from large, flat sheets, leading to significant material waste.[2] These factors contribute to the high cost of sandwich panels; it is estimated such components contribute to 30% of a wing mass, but 70% of the cost.[5]

Additive manufacture

One potential method for a reduction in production waste and improvement in lateral stiffness is employment of Additive Manufacture (AM) methods for core manufacture. AM has been used in industries requiring small numbers of specialized components for its ability to create net-shaped parts with geometries unsuitable for conventional manufacturing techniques; an example is the ability to create internal geometries unreachable through typical milling methods.[6] AM systems are suited for applications requiring a degree of customization, requirements for design optimization, and low production volumes.[7] Such qualities make AM an ideal candidate for

*Corresponding author, email d.pollard@bristol.ac.uk

Received 25 September 2016; accepted 2 March 2017
Doi:10.1080/20550340.2017.1306337

specialized and low-volume core components, and repair at facilities without access to traditional core materials.[8] These processes are broadly divided into three categories referring to the state of the initial build material; powder-based, extrusion-based, and resin-based,[9] with recent standards further subdividing the categories.[10] Each method has advantages and disadvantages, as discussed in Refs.[11,12]

An oft-highlighted issue with AM is the difficulty in quality control[6,13–16]; Huang et al.[16] present a thorough review of quality control in AM. Process parameter optimization allows design for improvements in manufacturing, as in,[17] and improved mechanical proper- ties.[18,19] However, there are relatively few methods of monitoring AM in use, with most relying on a single observation method.[16] Two case studies presented in[6] display qualification processes of AM parts for aerospace, with the manufacturing method motivated through reducing part weight; the first was qualified as a part, with no design variation allowed. The second involved process qualification, demonstrating print parameters which produce reliable components throughout the build space. The difference in certification requirements between a process and a design is reinforced through recent Food and Drug Administration (FDA) draft guidance, attempting to define the level of personalization for medical devices produced through AM, and the associated quality control processes.[20] Similar actions are required for part qualification for the aerospace industry, including standardization of material testing[21] and improved knowledge of the AM process to allow Non-Destructive Testing (NDT).[22] Within the aerospace industry, a number of parts have been qualified.[13,23]

Fused Deposition Modeling

Fused Deposition Modeling (FDM), a type of extrusion-based AM, is a technology pioneered by Stratasys Inc (now Stratasys Ltd) in 1992.[13,24] A typical FDM system involves extruding molten plastic through a nozzle, with actuation provided to move the nozzle relative to the print bed along a predefined path. The RepRap project began in 2008, providing open source designs for FDM machines.[25] Fused Deposition Modeling is a term trademarked by Stratasys, this process is synonymous to as Fused Filament Fabrication (FFF); the process is defined by ISO/ASTM 52900:2015 as material extrusion.[26] With the increased availability and ease of modification, costs of FDM systems have decreased, while the variety and application areas have increased. These attributes lead to an increased use within industry.[13]

Factors limiting adoption of FDM in industrial manufacturing is the difference in mechanical strength between an FDM and injection molded component, and the limited material choice available. Agarwala et. al.[27] investigated defects in FDM components, such as internal voids, the staircase effect, and start/stop errors. The anisotropic properties of FDM components in compression was explored by Lee et al.[28]; finding an 11.6% change in compressive strength dependent on part orientation. Tymrak et al.[29] found little difference in the mechanical properties of components manufactured on different machines. Many methods for improving the mechanical properties of the components have been suggested, such as the use of curved layers,[30,31] design optimization,[32,33] and process parameter optimization.[18,19,34,35] Material choice is limited by the melting point achievable by the extruder and viscosity during extrusion.

The bonding potential between layers of thin-walled AM components was explored by Yan et al.,[36] where the aspect ratio of a wall is related to the bond strength. The bonding potential was determined by the temperature difference between layers. Rodriguez et al. discuss the effect of temperature on bond strength; every 10 °C reduction in temperature difference between layers during extrusion corresponds to a 10% increase in fracture strength of the bond.[37] Most process optimization schemes modify parameters related to the infill of thicker components. The optimization of thin-walled FDM structures was presented by Riss et al.[38]

AM for core applications

While regular honeycomb core is relatively simple to manufacture in large sheets,[2] complex geometries commonly require multiple core types to be machined and spliced together. To date, there has been little research of AM technology applications in sandwich panel manufacture. In a patent filed in 2002, Boeing describes the use of thermoplastic honeycomb structures for use in radar cross sections produced using AM.[39] The listed advantages are increased manufacturing efficiency and improved design space over conventional cores. This concept has been explored by the University of Bristol,[8,40] investigating the mechanical properties of thermoplastic cores, the potential for use in repairing sandwich panels, and printing of cores onto curved surfaces. This line of research demonstrated sandwich panels can be printed *in situ* within a damaged section of sandwich panel, and directly onto prepreg material; a development which could allow for core manufacture and placement to take place simultaneously to streamline the production process. Allen and Trask[31] used a delta FDM machine to print curved layer cores. This process demonstrated the previous work can be applied to complex sandwich manufacture, and could be applied to complex panel repair. An application to composite sandwich structures has been explored by Riss et al.,[38] demonstrating the potential of manufacturing curved honeycomb structures through AM; modifying wall thickness within the CAD design to ensure reinforcement is in the loaded areas.

If sandwich panels are to improve in functionality within future aerospace and automotive applications, improved manufacturing methods will be required to achieve the "Bigger, Faster, Cheaper" mantra[41]; one potential method is to print lightweight cores through FDM. While previous work has provided an insight into the flexibility afforded to FDM cores, there has been little characterization of the thin wall mechanical strength, and comparison of such cores to existing core materials. FDM components exhibit anisotropic behavior, despite often comprising of homogeneous feed material, due to the layer-based manufacturing process. In contrast, Nomex honeycomb, manufactured from a phenolic paper-pulp, is a heterogeneous material, but produced with consistent wall dimensions and material properties due to mature manufacturing processes. The honeycomb core shape was chosen for the FDM core due to its efficient space filling with minimal volume.[42]

This paper begins with an investigation into the effect of different wall thicknesses and print speeds on the inter-layer bond strength of acrylonitrile butadiene styrene (ABS) and polylactic acid (PLA) manufactured with a RapMan 3.2 printer,[i] a low-cost printer used during this feasibility study. These

[i] Manufactured by BFB, now part of 3D Systems.

polymers are commonly used with such equipment; ABS is considered more suited for loaded components, while PLA provides a contrasting material to identify if similar trends were observed.[43] Following these results, FDM cores were manufactured and tested to evaluate the effect of different build patterns. An initial cost comparison between ABS cores produced through FDM with conventional Nomex honeycomb cores follows. The results are discussed, presenting a theory regarding the causes of result variability, succeeded by conclusions and further work.

Bond strength evaluation

A dominating factor in the mechanical strength of FDM components is the inter-layer bond strength.[19,44] Construction of walls through a single extruder pass allows for the lightest structures for core use; this research was conducted to understand the effects of print parameters on the thin wall strength. Tests were performed based on ASTM D638[45] to investigate the effects of varying build parameters on interlayer bond strength of ABS and PLA polymers.

Manufacture of tensile specimens

Wall thickness variations were introduced through variation of the nozzle speed and the material flow rate to observe the effect of increased manufacturing speeds. The printer was located in a research laboratory, with the build area at room temperature and normal humidity. Tests were performed with ABS and PLA plastics. For ABS, three extruder flow rates were considered (4.08, 5.44, 6.80 $mm^3 s^{-1}$), with nozzle speed settings to produce wall thicknesses (1.5, 2, 2.5 mm). Due to the lower viscosity of PLA, the same wall thicknesses were not achievable; two flow rates of 4.76 and 9.51 $mm^3 s^{-1}$ were used to manufacture walls of approximately 0.9 and 1.7 mm. Additional PLA specimens were produced with a 13 s pause time between layers to investigate the effect of increased cooling on filament bonding.

After printing, the thin walls were machined into hourglass specimens. Specimens were 50 mm long with a gauge length of 9 mm, and a width of 7 mm. The inter specimen variation of the gauge lengths and widths was 1 and 0.5 mm, respectively. The specimens were orientated within tensile testing mounts to ensure the loading direction was perpendicular to the layer line. Figure 2(a) shows a test specimen mounted in position for a tensile testing. Figure 2(b) depicts a typical failure observed during testing; a clean break along between layers normal to the direction of applied force.

Tensile testing results

Testing was conducted at a rate of 2 mm/min on a Shimadzu test machine, measured with a 1 kN load cell sampled at 100 Hz. From the peak force before failure, the ultimate tensile stress for each wall thickness was calculated using measurements for sample width and thickness. The results are shown in Table 1 for ABS, and Table 2 for PLA. The initial results show no statistically significant difference in ultimate tensile stress for variations in extruder flow rate and wall thickness. It was observed the thicker specimens were more likely to fail out of gauge length; any failure outside of the gauge length was discounted from results. Of the 100 specimens tested, with 14 failing during machining or outside of the gauge length.

Table 1 Ultimate tensile stress (MPa) for wall thickness and flow rate variations of ABS samples

		Wall thickness (mm)		
		1.5	2.0	2.5
Flow rate ($mm^3 s^{-1}$)	4.08	24.2 ± 1.3	26.1 ± 2.4	24.1 ± 2.4
	5.44	25.2 ± 3.8	26.3 ± 4.1	22.1 ± 2.1
	6.80	24.7 ± 3.9	25.9 ± 4.1	22.9 ± 1.8

Table 2 Ultimate tensile stress (MPa) for wall thickness and flow rate variations of PLA samples. The sample group with a longer pause time is represented in italics

		Wall thickness (mm)		
		0.9	*0.9*	1.7
Flow rate ($mm^3 s^{-1}$)	4.73	21.2 ± 2.7	–	23.9 ± 2.1
	9.51	24.6 ± 1.1	25.6 ± 1.4	18.3 ± 4.3

Appendix 1 shows the force–displacement curve for each specimen, with the yield points marked by black squares. Also presented are the results for samples with an increased layer print time through addition of the 13 s pause, compared to identical parameters with a default layer time.

It can be seen the thinner-walled structures printed with ABS behave in a more brittle way than the thicker walled samples; exhibiting a shorter yield before failure. It can be hypothesized from the higher amount of plastic deformation, identified on the tensile testing graphs in Appendix 1, the specimen behaves closer to that expected for a conventionally manufactured plastic specimen; implying a higher level of inter-layer bonding than exhibited in the thinner-walled structures.

Due to increased contact area between filaments in thicker walls from the wider roads deposited, a heat gradient during the bond-forming process would exist across the road width, with the edge section cooling at a higher rate due to convection. As the entanglement between the polymer layers is related to the cooling profile, a higher level of entanglement is exhibited in the center of the bond relative to the edge.[44] With the lower level of bonding at the edge, a peeling action may occur, causing the earlier yield point observed. The thinner walls would be expected to have a more uniform temperature along the filament bond, the yield point is reached closer to failure with minimal peeling between layers.

From Fig. 8, it can be seen there is an increase in the spread of ultimate tensile force when the layer time is increased through the pause, while the yield point remains constant. While there is no significant statistical difference in yield or ultimate tensile stress, it can be seen there is a high variation in displacement at ultimate failure. The cause of these changes in ultimate strain could be environmental effects during the pause; this variable has a great effect on bonding on bonding, as discussed in Refs. 36 and 37.

Compressive testing of cores

ABS cores were manufactured through FDM using various toolpaths; each resulting in different wall thicknesses. These were compared to Nomex honeycomb and PLA core

Table 3 Specimen wall thickness and build properties

Wall type	Thickness (mm)	Normalized thickness	Expected normalized thickness	Build time (min)
1	0.56	1	1.00	41.0
2	0.79	1.42	1.33	47.8
3	1.11	1.98	2.00	69.8
PLA	0.85	1.35	1.33	47.9
Nomex	0.08	–	1.33	–

specimens. *A* honeycomb build pattern was selected, due to the efficiency of honeycomb as a filling pattern and the resemblance to Nomex honeycomb. The test design was based on ASTM D7336.[46]

Manufacture of the FDM cores

Custom code was created within the MATLAB environment to output a GCode file directly to the 3D printer, enabling control over the print toolpath, flow rate, and nozzle speed. Three different build profiles were investigated for the ABS specimens, shown in Fig. 3. Testing of the cores manufactured from PLA was limited to those produced using toolpath 2, the most reliable toolpath. The built properties are described in Table 3, with the wall thicknesses, normalized, and expected normalized thicknesses stated. The expected normalized thickness values were calculated from the amount of repeated printing of the hexagon walls. Toolpath 3 is identical to the output of the default RapMan slicing software (Axon 3).

Examples of the FDM and Nomex honeycomb cores used for this testing are shown in Fig. 4(a) and (b), in Appendix 2. A5 mm cell radius was used for the FDM core, and a 1.6 mm cell radius for Nomex honeycomb. The Nomex honeycomb had a density of 48 kg m^{-3}. FDM specimens were printed to a size of $50 \times 50 \times 14 \pm 1$ mm, and the Nomex honeycomb core cut with a bandsaw from a 14 mm depth sheet to $50 \times 50 \pm 2$ mm. This specimen size was similar to those used by Zhang and Ashby when evaluating the theoretical compressive strength of Nomex honeycomb.[47]

Compressive testing results

Testing was conducted on level plates mounted on a 50 kN Zwick test machine at a rate of 2 mm/min, sampled at 10 Hz. The cores were preloaded to 50 N, and the plates were checked to ensure the orientation was correct. Table 4 presents the yield force, yield and crush stress, and specific crush stress for each build pattern. The specific crush stress was calculated by dividing the ultimate crush force by specimen mass. In a similar result to the tensile results presented in Section Bond strength evaluation, the thinner walled core behaves in a more brittle manner than the thick-walled counterparts, with little plastic deformation occurring between yield and crush stresses.

Figure 5 shows force–displacement curves normalized by the ultimate failure load for compression testing of the ABS and Nomex honeycomb cores. The results for individual tests are shown in Appendix 2. While the Nomex honeycomb follows the anticipated crushing behavior with a constant crush force,[47] the FDM cores followed a more typical buckling behavior for plastic structures. The FDM cores withstood a significantly higher force before failure than Nomex honeycomb,

Table 4 Force and stress of walls crush testing of different deposition patterns for FDM and Nomex honeycomb cores.

Wall type	Yield force (kN)	Yield stress (MPa)	Crush stress (MPa)	Specific yield stress (MPa/g)
1	9.1 ± 0.3	18.9 ± 1.1	21.6 ± 1.5	4.0 ± 0.2
2	20.1 ± 0.7	29.6 ± 2.8	35.2 ± 2.4	4.8 ± 0.4
3	33.2 ± 0.4	34.5 ± 1.0	40.0 ± 1.1	3.7 ± 0.1
PLA	32.8 ± 1.2	42.9 ± 2.6	51.1 ± 3.2	5.0 ± 0.2
Nomex	5.4 ± 0.1	36.6 ± 1.0	41.2 ± 0.7	19.1 ± 0.5

with similar crush stresses. Due to the increased mass of the FDM core, the specific crush stress is much lower. The higher compressive strength of the PLA specimen corresponds to the findings of Tymrak et al.[29]

With a more brittle thin-walled structure, there was little deformation before buckling. This failure mode was exhibited through separation between layers, with the layers remaining relatively undistorted. The increased ductility of this bond, as discussed in Section Bond strength evaluation, resulted in the more ductile core failure. With the increased contact area and ductile deformation, *a* significantly higher force was required to reach peak deformation. The post-failure behavior, shown by the force–displacement compression graphs in Fig. 5, shows the increased resistance to crushing after the initial failure; plastic behavior similar to that presented in Section Tensile testing results.

The deposition pattern also introduced anisotropic properties to the core. As discussed in Refs.,[1,2] traditional Nomex honeycomb exhibits anisotropic properties due to the impregnated paperbased materials; there is very little lateral compressive stiffness. FDM exhibits anisotropic properties due to the layered manufacturing approach,[19] but due to the higher compressive stiffness of the ABS compared to the paperbased Nomex honeycomb, there is no noticeable difference when handled in different orientations. This would be beneficial for ensuring geometric tolerances are maintained during layup of the upper skin of sandwich panels. Existing thermoplastic cores offer improved lateral stiffness compared to Nomex honeycomb, and have a maximum compressive strength of 1.9 N mm^{-2} (Ref. 48). With a compressive strength of 3.9 N mm^{-2}, the ABS core printed with toolpath 1 was stronger, and had twice the density.

Cost comparison

An approximate cost comparison has been conducted, investigating the material cost difference between ABS printed cores and an aerospace grade Nomex honeycomb core. A sheet of Nomex core (121.9 × 243.8 × 2.5 mm) costs between $927 and $2663.[49] Printing the same volume of core using toolpath 2, shown in Fig. 3, as the Nomex honeycomb would weigh 13.44 kg. This paper uses filament priced at $21 per kilogram, purchased from 3D Filaprint,[50] equating to a cost of $282 for an equivalent area of core with a depth of 2.5 mm; a factor of between 4 and 10 lower cost than Nomex honeycomb. This analysis does not take into account the machining costs for producing more complex geometries; an aspect where the FDM process would have reduced waste and a higher level of automation due to the nature of the AM process.

(a) Complex core shape produced through FDM with top and bottom skins

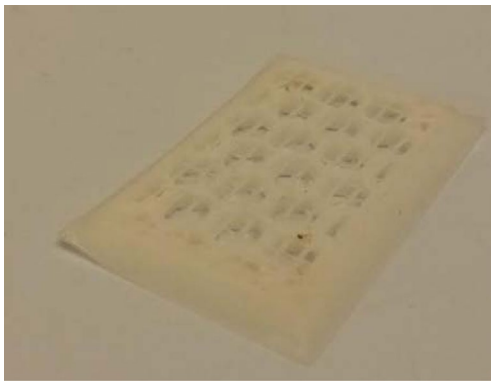

(b) Core produced through FDM with a mesh cell printed to prevent top skin deformation during curing

Figure 1 Example cores produced through FDM[40]

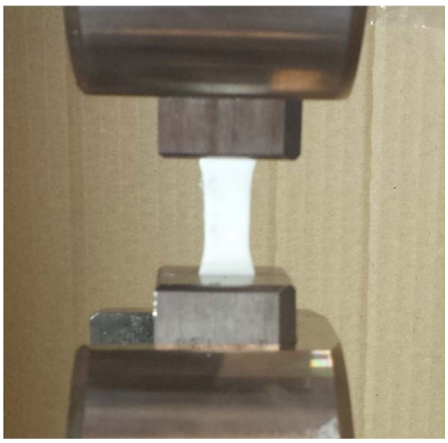

(a) Test specimen mounted in tensile test rig. The end tabs were secured directly to the test machine, and the top gripper could freely rotate to ensure no torsional forces were applied

(b) Test specimen after failure. This depicts a typical failure, with a clean break along the layer line

Figure 2 Thin-walled test specimens used for tensile testing. (a) A specimen mounted in the test rig, (b) the fracture during failure along the inter-layer bond

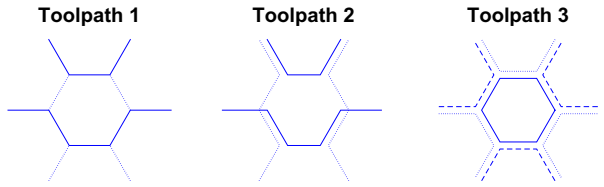

Figure 3 The pictorial representation of the three toolpaths investigated, depicted for the construction of a single hexagon cell. The lines are offset to show each pass on for the edges of the honeycomb cell. Each line of continuous extrusion is represented by a different dash type.

Discussion

Section Bond strength evaluation presented inter-layer bond failure mechanisms for different wall thicknesses; the thicker walls behaved in a more ductile manner. In Section Compressive testing of cores, it can be seen that the FDM cores exhibit a higher compressive force, and a lower specific strength than the Nomex honeycomb used in this work. The cores manufactured through FDM had a higher compressive strength than thermoplastic polymer cores, and an increased density, demonstrating equivalence to existing industrial materials. Wall thickness was found to be a contributing factor to the difference between the yield and ultimate displacements. However, with the increased crush force after failure of the plastic cores, there is potential for improved impact resistance.[8] Through correlation between Sections Bond strength evaluation and Compressive testing of cores, it can be concluded that interlayer bond strength is key in determining the failure properties of the final core.

There are advantages to the use of FDM cores in secondary structures, where low cost and ease of manufacturing are a priority; especially when complex geometries are common. Here, the core strength could be optimized for areas with high localized loads (e.g. inserts) through modification of the deposition pattern and wall thickness; properties could be identified through the testing presented in Section Bond strength

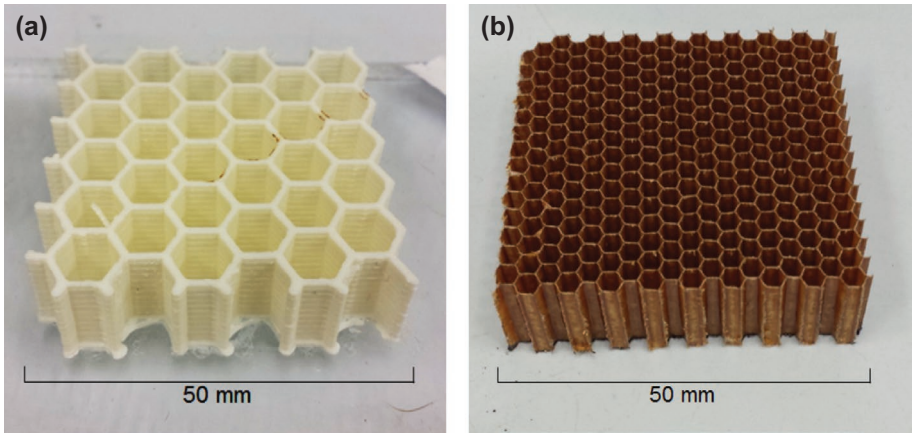

Figure 4 Cores used during testing. (a) An example core of ABS manufactured through FDM, as used within this paper. (b) A Nomex honeycomb core of the same size; the difference in cell size due to the manufacturing limitations of the FDM process is clear

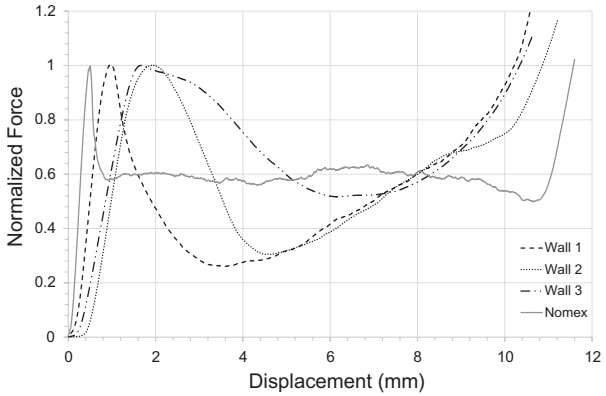

Figure 5 Normalized force–displacement curves for ABS printed cores (dashed lines) and the Nomex honeycomb core (solid line). The force is normalized to the ultimate load to show the varying failure behaviors between core types

evaluation. Using a combination of Nomex and metallic honeycomb to form complex geometry requires careful machining and splicing.[1] With FDM, extra complexity in manufacturing is available at virtually no extra cost.[6] In addition to the ability to support localized loads, AM allows more complex designs to be produced than possible with conventional sandwich panels. An example is shown in Fig. 1(a), from previous work.[40]

A number of quality control issues were identified during the specimen manufacture and data acquisition. One observation of this paper was the increased variation in yield point for FDM parts produced with thicker walls. In addition, the thicker walled specimens have been found to be more susceptible to errors during manufacture; as stated in Section Manufacture of tensile specimens. It was observed the print quality was dependent on the initial layer height; while a constant layer height was used, having the initial layer deposited too low could cause "ripples" throughout the component. This effect caused such specimens to be discarded before machining.

There was a difference of an order of magnitude between the cell sizes and wall thicknesses of the FDM and Nomex honeycomb cores. The larger cell size of the FDM cores present a risk of "telegraphing"; where the top skin vertically deforms into the cell. This could be countered through printing a shell structure over the top, as shown in Fig. 1(b).

Conclusion and further work

This paper has presented the results of testing filament bond strength of thin-walled honeycomb cores produced with two differing materials (ABS and PLA) using FDM. Testing was conducted with samples machined from FDM thin walls for bond strength evaluation through tensile testing. Results have shown thicker walls are more susceptible to plastic deformation, with a lower yield point than thinner walls. Compressive testing of the FDM cores has demonstrated the thicker walled specimens behaved in a more ductile way, consistent with the tensile testing; the maximum crush force of the FDM cores was significantly greater than Nomex honeycomb. While the specific compressive strength remains roughly constant with wall thickness variations, it is lower than Nomex honeycomb, a barrier to use in weight-critical applications. A second advantage of core components manufactured through FDM is the improved design envelope, reducing manufacturing limitations imposed by conventional machining.

Future work will involve further testing of FDM cores in impact and torsion. With the wider design space the FDM process provides, alternative structures achievable through FDM will be explored. In addition, printer types with alternative materials, such as carbon reinforced filaments, will be investigated.

Acknowledgments

The authors would like to thank Ed Cooper for his assistance in gathering data.

Funding

This work was supported by the EPSRC Centre for Doctoral Training in Future Autonomous Robotic Systems (FARSCOPE) at the Bristol Robotics Laboratory [grant number EP/L015293/1]. All underlying data are provided in full within this paper.

Disclosure statement

No potential conflict of interest was reported by the authors.

ORCID

J. Etches http://orcid.org/0000-0001-8848-7746

References

1. D. Zenkert: 'An introduction to sandwich construction', 1997, Sheffield, Engineering Materials Advisory Services.
2. T. Bitzer: 'Honeycomb technology', 1997, Springer Science & Business Media.
3. C. Ward, K. Hazra and K. Potter: 'Development of the manufacture of complex composite panels,' *Int. J. Mater. Prod. Technol.*, 2011, **42**, (3–4), 131–155.
4. K. Potter: 'Achieving low variability, rework and scrap rates in the production of advanced composite parts', SEICO09, SAMPE Europe30th, 2009.
5. R. Melville: 'Introduction to NGCW and the future product perspective', Lavaur, Fr: Airbus SAS, 2007.
6. N. Hopkinson, R. Hague and P. Dickens: 'Rapid manufacturing: an industrial revolution for the digital age', 2006, Chichester, Wiley.
7. S. Mellor, L. Hao and David Zhang: 'Additive manufacturing: A framework for implementation,' *Int. J. Prod. Econ.*, 2014, **149**, 194–201.
8. J. White, J. Etches and C. Ward: 'CDE 28088: The development of low cost additive layer manufacturing for use as repair equipment in the field, to improve operations and support for composite platforms', Technical report, Bristol, University of Bristol, 2013.
9. J.-P. Kruth: 'Material incress manufacturing by rapid prototyping techniques,' *CIRP Ann. Manuf. Technol.*, 1991, **40**, (2), 603–614.
10. ASTM F2792-12a: 'Standard terminology for additive manufacturing technologies, (withdrawn 2015)', 2012, West Conshohocken, PA, ASTM International.
11. D. Dimitrov, K. Schreve and N. de Beer: 'Advances in three dimensional printing-state of the art and future perspectives,' *Rapid Prototyping J.*, 2006, **12**, (3), 136–147.
12. W. Gao, Y. Zhang, D. Ramanujan, K. Ramani, Y. Chen, C. B. Williams, C. C. L. Wang, Y. C. Shin, S. Zhang and P. D. Zavattieri: 'The status, challenges, and future of additive manufacturing in engineering,' *Comput. Aided Des.*, 2015, **69**, 65–89.
13. T. Wohlers and T. Caffrey: 'Wohlers report 3D printing', 2013, Fort Collins, CO, Wohlers Associates.
14. W. Oropallo and L. A. Piegl: 'Ten challenges in 3D printing,' *Eng. Comput.*, 2016, **32**, (1), 135–148.
15. G. Tapia and A. Elwany: 'A review on process monitoring and control in metal-based additive manufacturing,' *J. Manuf. Sci. Eng.*, 2014, **136**, (6), 060801.
16. T. Huang, S. Wang, and K. He: 'Quality control for fused deposition modeling based additive manufacturing: Current research and future trends', First Int. Conf. on 'Reliability Systems Engineering' (ICRSE), 2015, Beijing, IEEE, 1–6.
17. G. Pavan Kumar and S. Prakash Regalla: 'Optimization of support material and build time in fused deposition modeling (FDM),' *Appl. Mech. Mater.*, 2012, **110**, 2245–2251.
18. F. Rayegani and G. C. Onwubolu: 'Fused deposition modelling (FDM) process parameter prediction and optimization using group method for data handling (GMDH) and differential evolution (DE),' *Int. J. Adv. Manuf. Technol.*, 2014, **73**, (1–4), 509–519.
19. O. Mohamed, S. Masood and J. Bhowmik: 'Optimization of fused deposition modeling process parameters: a review of current research and future prospects,' *Adv. Manuf.*, 2015, **3**, (1), 42–53.
20. Food and Drug Administration: 'Technical considerations for additive manufactured devices', 2016, Silver Spring, MD, Draft Guidance for Industry and Food and Drug Administration Staff.
21. Y. Huang, M. C. Leu, J. Mazumder and A. Donmez: 'Additive manufacturing: current state, future potential, gaps and needs, and recommendations,' *J. Manuf. Sci. Eng.*, 2015, **137**, (1), 014001.
22. P. A. Kobryn, N. R. Ontko, L. P. Perkins and J. S. Tiley: 'Additive manufacturing of aerospace alloys for aircraft structures', Technical report, DTIC Document, Wright-Patterson Air Force Base, USA, 2006.
23. N. Guo and M. C. Leu: 'Additive manufacturing: technology, applications and research needs,' *Front. Mech. Eng.*, 2013, **8**, (3), 215–243.
24. S. S. Crump: 'Apparatus and method for creating three-dimensional objects', US Patent 5121329, 9 June 1992.
25. R. Jones, P. Haufe, E. Sells, P. Iravani, V. Olliver, C. Palmer and A. Bowyer: 'RepRap – the replicating rapid prototyper,' *Robotica*, 2011, **29**, (1), 177–191.
26. 'Additive manufacturing – General principles – Terminology', ISO/TC 261, ISO/ASTM 52900:2015, Berlin, Germany.
27. M. Agarwala, V. Jamalabad, N. Langrana, A. Safari, P. Whalen and S. Danforth: 'Structural quality of parts processed by fused deposition,' *Rapid Prototyping J.*, 1996, **2**, (4), 4–19.
28. C. Lee, S. Kim, H. Kim and S. Ahn: 'Measurement of anisotropic compressive strength of rapid prototyping parts,' *J. Mater. Process. Technol.*, 2007, **187**, 627–630.
29. B. Tymrak, M. Kreiger and J. Pearce: 'Mechanical properties of components fabricated with open-source 3-d printers under realistic environmental conditions,' *Mater. Des.*, 2014, **58**, 242–246.
30. S. Singamneni, A. Roychoudhury, O. Diegel and B. Huang: 'Modeling and evaluation of curved layer fused deposition,' *J. Mater. Process. Technol.*, 2012, **212**, (1), 27–35.
31. R. Allen and R. Trask: 'An experimental demonstration of effective curved layer fused filament fabrication utilising a parallel deposition robot,' *Addit. Manuf.*, 2015, **8**, 78–87.
32. O. Stava, J. Vanek, B. Benes, N. Carr and R. Měch: 'Stress relief: improving structural strength of 3*D* printable objects,' *ACM Trans. Graphics*, 2012, **31**, (4), 48.
33. A. Garland and G. Fadel: 'Design and manufacturing functionally gradient material objects with an off the shelf three-dimensional printer: challenges and solutions,' *J. Mech. Des.*, 2015, **137**, (11), 111407.
34. A. Garg, K. Tai and M. M. Savalani: 'State-of-the-art in empirical modelling of rapid prototyping processes,' *Rapid Prototyping J.*, 2014, **20**, (2), 164–178.
35. S. Guessasma, W. Zhang, J. Zhu, S. Belhabib and H. Nouri: 'Challenges of additive manufacturing technologies from an optimisation perspective,' *Int. J. Simul. Multidisci.*, 2015, **6**, A9.
36. Y. Yan, R. Zhang, G. Hong and X. Yuan: 'Research on the bonding of material paths in melted extrusion modeling,' *Mater. Des.*, 2000, **21**, (3), 93–99.
37. J. F. Rodriguez, J. P. Thomas and J. E. Renaud: 'Characterization of the mesostructure of fused-deposition acrylonitrile-butadiene-styrene materials,' *Rapid Prototyping J.*, 2000, **6**, (3), 175–186.
38. F. Riss, J. Schilp and G. Reinhart: 'Load-dependent optimization of honeycombs for sandwich componentsnew possibilities by using additive layer manufacturing,' *Phys. Procedia*, 2014, **56**, 327–335.
39. M. Hayes, J. DeGrange, C. Rice and J.Polus: 'Honeycomb cores for aerospace applications', US Patent App. 10/236361, 6 September 2002.
40. D. Pollard: 'Automated sandwich panel production utilising additive manufacture and silicone pick and place technology', Master's thesis, University of Bristol, Bristol, June 2014.
41. J. E. C. Composites: 'Bigger, faster, cheaper,' *JEC Compos. Mag.*, 2014, **86**, 23–24.
42. Q. Zhang, X. Yang, P. Li, G. Huang, S. Feng, C. Shen, B. Han, X. Zhang, F. Jin, F. Xu, and T. Lu: 'Bioinspired engineering of honeycomb structure using nature to inspire human innovation,' *Prog. Mater. Sci.*, 2015, **74**, 332–400.
43. M. Dawoud, I. Taha and S. J. Ebeid: 'Mechanical behaviour of abs: An experimental study using FDM and injection moulding techniques,' *J. Manuf. Proc.*, 2016, **21**, 39–45.
44. Q. Sun, G. Rizvi, C. Bellehumeur and P. Gu: 'Effect of processing conditions on the bonding quality of FDM polymer filaments,' *Rapid Prototyping J.*, 2008, **14**, (2), 72–80.
45. ASTM D638-14: 'Standard test method for tensile properties of plastics', 2014, West Conshohocken, PA, ASTM International, Available at www.astm.org.
46. ASTM D7336 / D7336M-16: 'Standard test method for static energy absorption properties of honeycomb sandwich core materials', 2016, West Conshohocken, PA, ASTM International.
47. J. Zhang and M. F. Ashby: 'The out-of-plane properties of honeycombs,' *Int. J. Mech. Sci.*, 1992, **34**, (6), 475–489.
48. Plascore: 'PC2 polycarbonate honeycomb', 2014, Available at http://www.plascore.com/download/datasheets/honeycomb-data-sheets/Plascore-PC2.pdf, (accessed [15 February 2017]).
49. Professional Plastics: 'Nomex honeycomb', 2017, Available at [http://www.professionalplastics.com/Nomex-Honeycomb], (accessed [27 January 2017]).
50. 3DFilaprint: '2.85/3 mm ABS filament', 2017, Available at [http://shop.3dfilaprint.com/285mm3mm-357-c.asp], (accessed [27 January 2017]).

Appendix 1.

Force–displacement of tensile tests (overleaf).

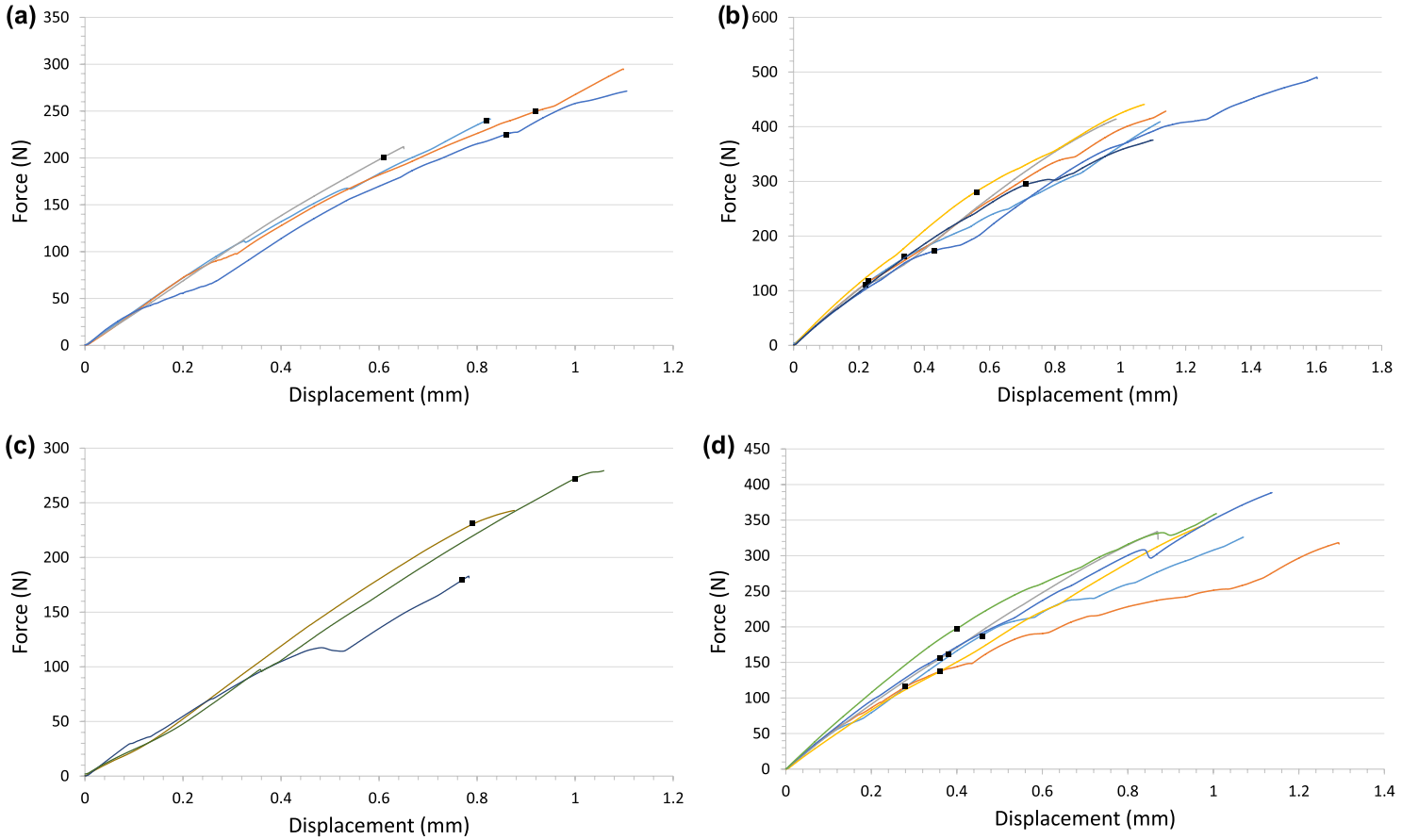

Figure 6 Force–displacement curves for ABS tensile samples. The yield points for each specimen are identified by a black square; this point was determined through the decrease in gradient at the end of the region of linear deformation. The parameters used for each test are: (a) 1.5 mm wall, 4.08 mm³ s⁻¹ flow rate, (b) 2.5 mm wall, 4.08 mm³ s⁻¹ flow rate, (c) 1.5 mm wall, 6.80 mm³ s⁻¹ flow rate, (d) 2.5 mm wall, 6.80 mm³ s⁻¹ flow rate

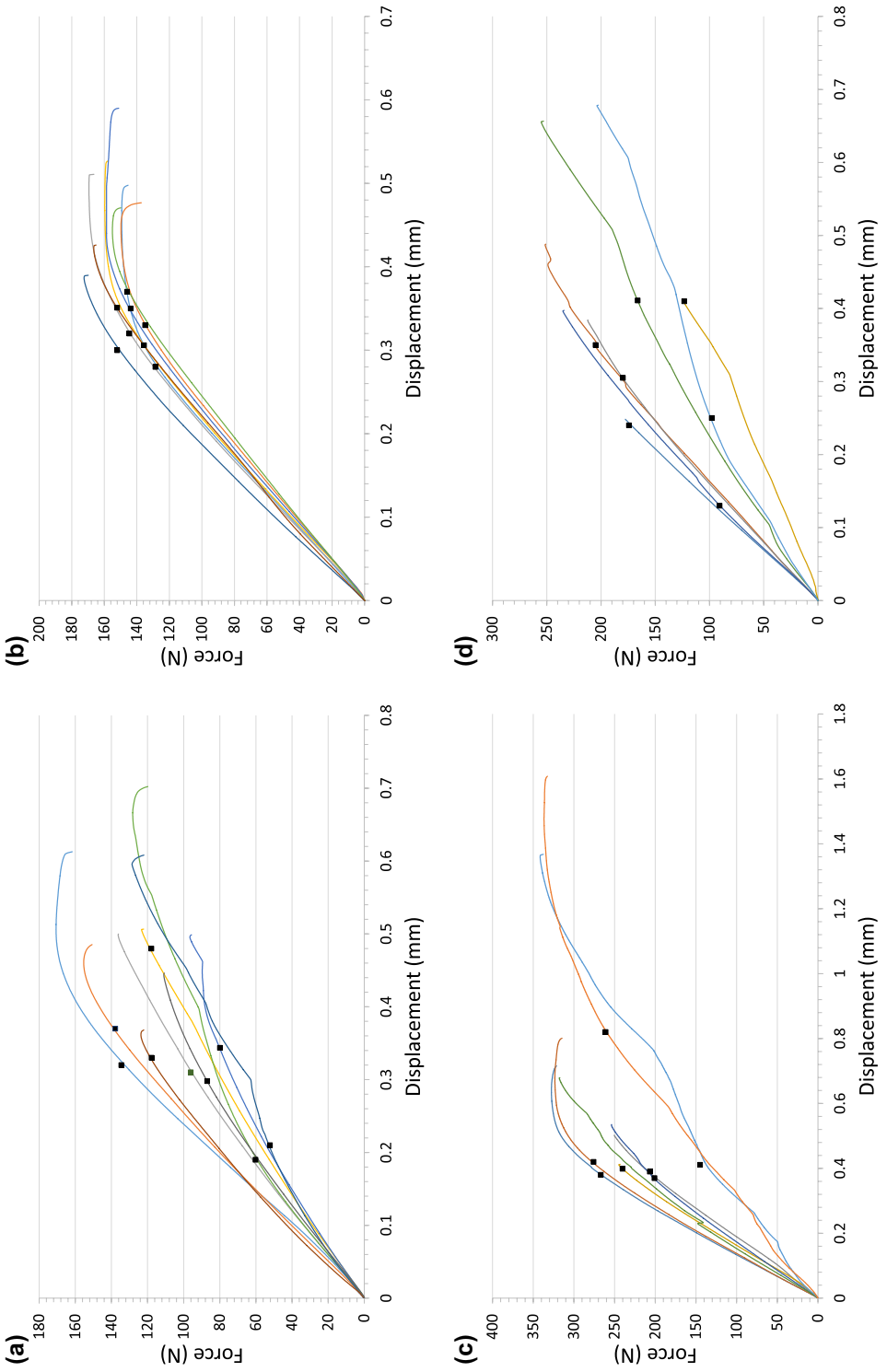

Figure 7 Force–displacement curves for PLA tensile samples. The yield points for each specimen are identified by a black square; this point was determined through the decrease in gradient at the end of the region of linear deformation. The parameters used for each test are: (a) 0.9 mm wall, 4.73 $mm^3 s^{-1}$ flow rate, (b) 1.7 mm wall, 4.73 $mm^3 s^{-1}$ flow rate, (c) 0.9 mm wall, 9.51 $mm^3 s^{-1}$ flow rate, (d) 1.7 mm wall, 9.51 $mm^3 s^{-1}$ flow rate.

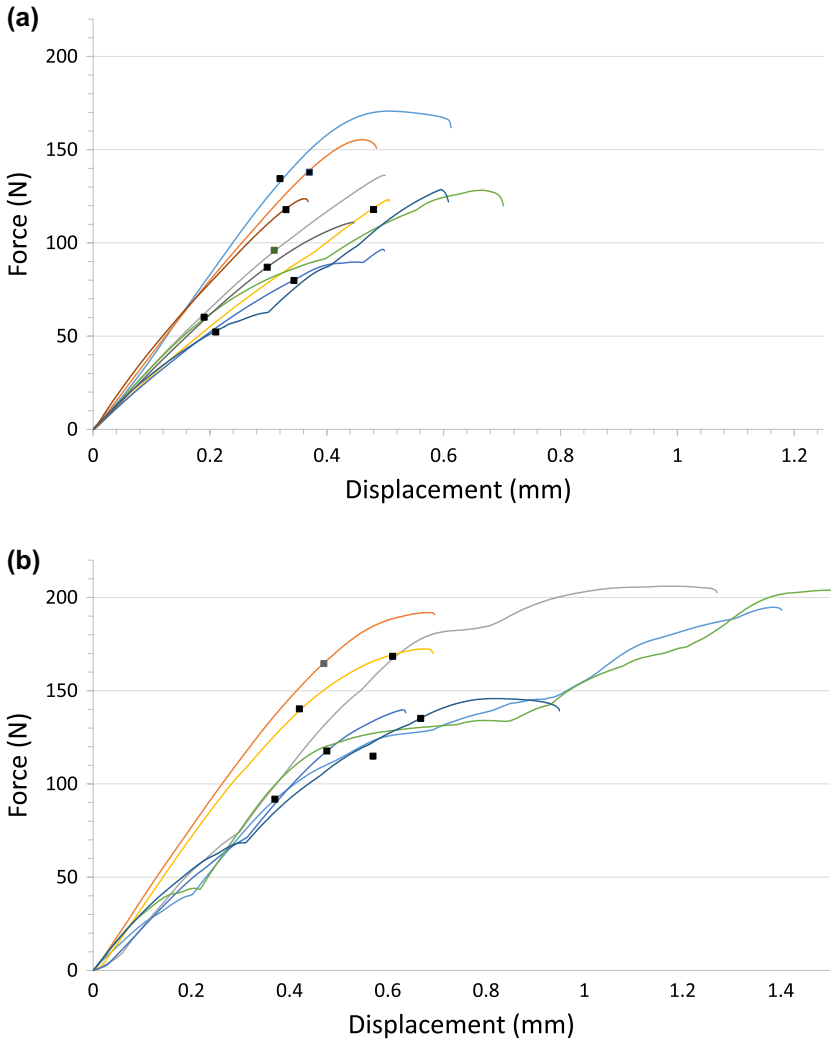

Figure 8 Force–displacement curves for PLA tensile specimens printed with differing layer times. The black squares represent the yield points of the specimens, found through observation of the end of the elastic region of the force{displacement curve. (a) was printed with the same parameters as Figure 7a, while (b) had a 13 s pause applied

Appendix 2.

Force–displacement of core compression tests.

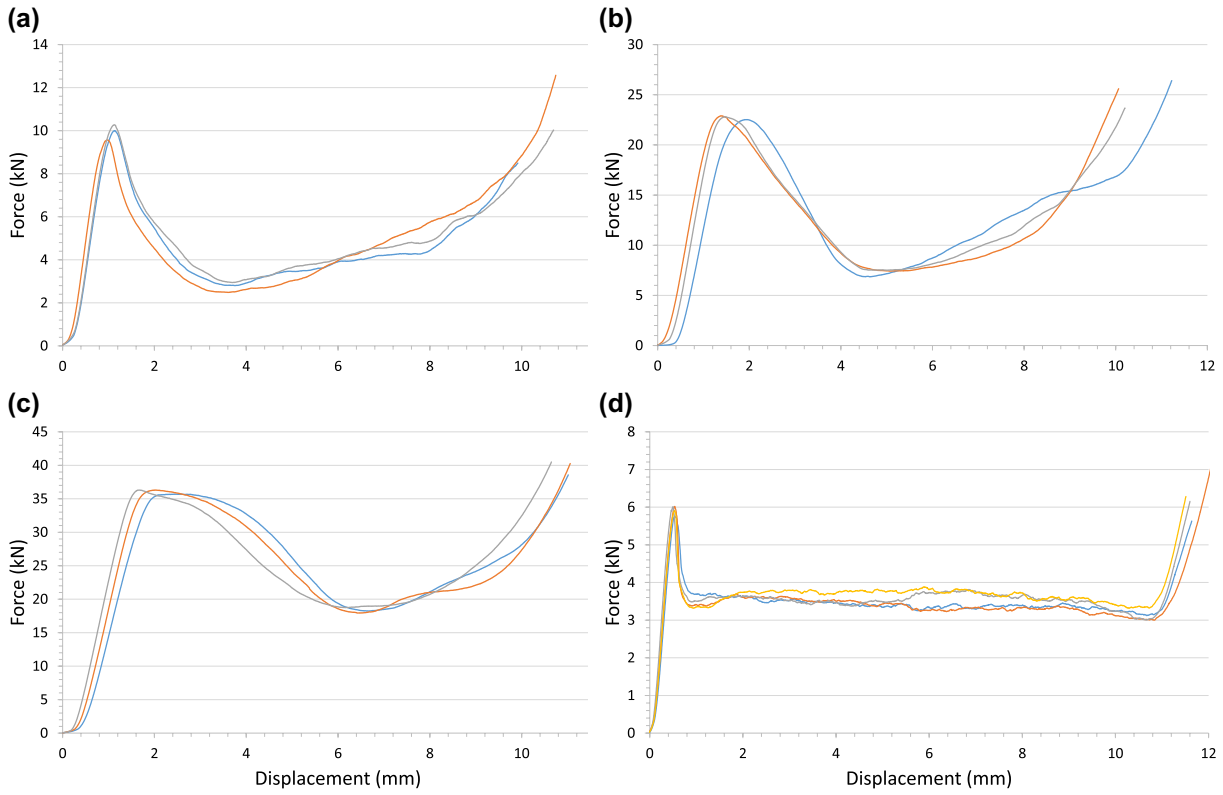

Figure 9 Force–displacement curves for compressive testing of ABS cores produced through Fused Deposition Modeling (FDM). (a) was manufactured using toolpath 1, as described in Figure 3. (b) and (c) were manufacturing using toolpaths 2 and 3 respectively. (d) is a Nomex honeycomb core, with a cell size 3.2 mm and density 48 kg m^{-3}, commonly used within the aerospace industry